u!nnovation.

UNITED IMAGING

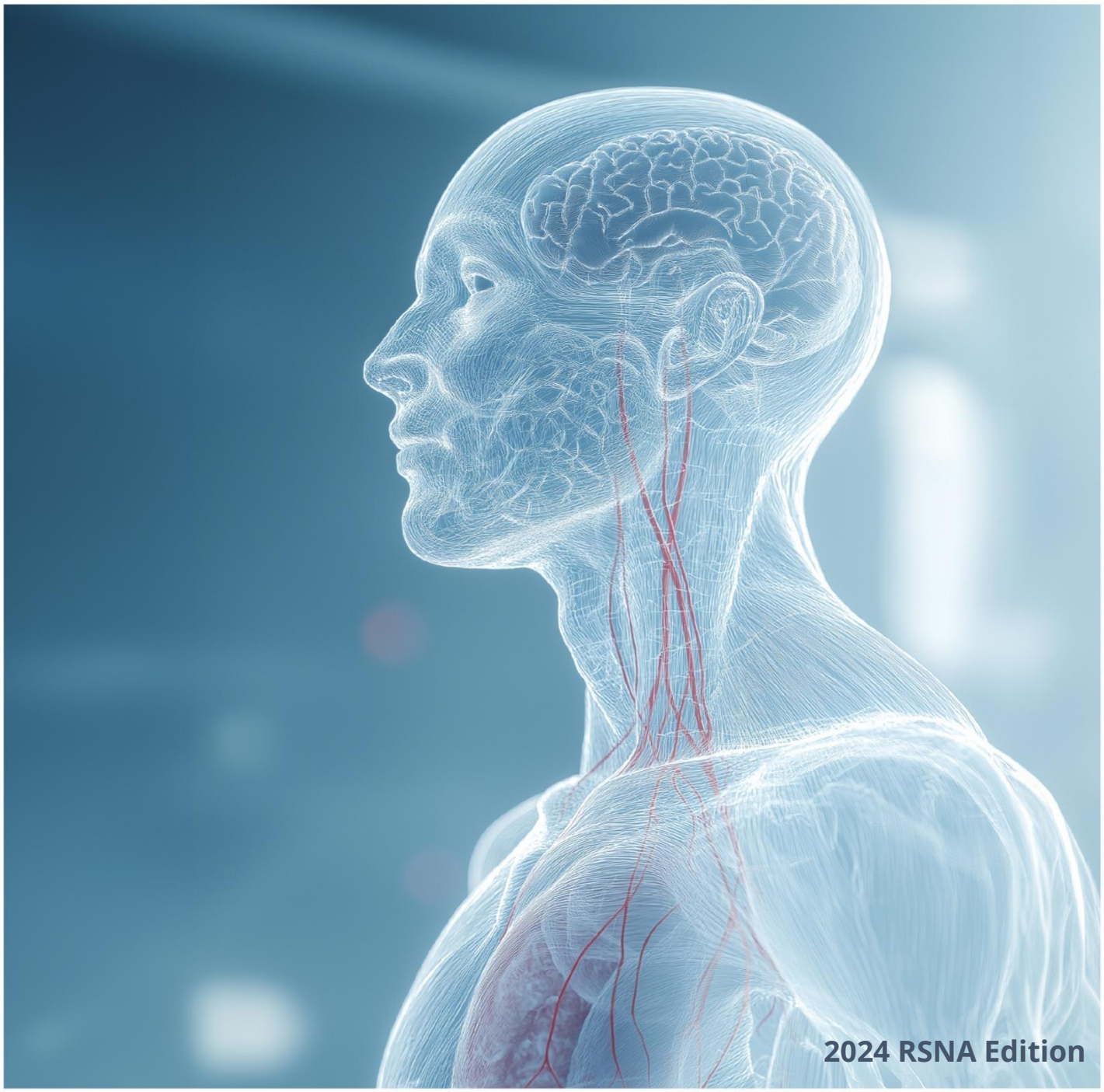

Issue Highlights

[Unveiling the Mind: Journeying through Brain PET with Dr. Richard E. Carson](#)

Edwin K. Leung

Page 25

[An AI-Empowered Head-Only Ultra-High-Performance Gradient MRI System for High Spatiotemporal Neuroimaging](#)

Liyi Kang et al.

Page 44

[5T MRI Compared to 3T MRI in Routine Brain Imaging: An Evaluation of Image Quality](#)

Zhensong Wang et al.

Page 53

[One-stop dynamic whole-brain CT perfusion with a 320-row scanner for patients with acute ischemic stroke and the clinical value of artificial intelligence iterative reconstruction](#)

Jin Fang et al.

Page 64

Disclaimer

The articles contained in this magazine are provided solely by the authors, and the author(s) of each article appearing in this magazine is/are solely responsible for the content thereof as well as personal data, which is used anonymously or complied with applicable data privacy laws or regulations. United Imaging Healthcare makes no representation or warranties, expressly or impliedly, with respect to the accuracy, timeliness, reliability, legitimacy, applicability, fitness, originality, or completeness of the contents of this magazine. United Imaging Healthcare assumes no legal responsibility or liability for any error, omission, or illegality with respect to the material contained within.

All articles contained in this magazine only represent the opinions and views of the authors and do not implicitly or explicitly represent any official positions or policies, or medical opinions of United Imaging Healthcare or the institutions with which the authors are affiliated unless this is clearly specified. Discussions of any brand, services, or products in the magazine should not be construed as promotion or endorsement thereof.

Articles published in this magazine are intended to inspire further general scientific research, investigation, understanding, and discussion only and are NOT intended to and should not be relied upon as recommending or promoting a specific medical advice, method, diagnosis, or treatment by physicians for any particular individual, nor to replace the advice of a medical doctor or other healthcare professional. Any individual wishing to apply the information in this magazine for the purposes of improving their own health should not do so without consulting with a qualified medical practitioner. All patients need to be treated in an individual manner by their personal medical advisors. The decision to utilize any information in this magazine is ultimately at the sole discretion of the reader, who assumes full responsibility for any and all consequences arising from such a decision. United Imaging Healthcare makes no representations or warranties with respect to any treatment, action, or application of medication or preparation by any person following the information offered or provided within or through the magazine. United Imaging Healthcare shall remain free of any fault, liability, or responsibility for any loss or harm, whether real or perceived, resulting from the use of information in this magazine.

The articles included in this magazine may contain work in progress, which represents ongoing research and development. Such technologies are not available for sale in the United States for clinical use and also may not be available for such sales in other countries around the world.

Please note that the magazine is intended to be distributed only within a limited scope instead of publication.

If you have any questions about the magazine, or simply wish to reach out to us for any other reasons, you are welcomed to contact us at the following email address: compliance@united-imaging.com

Clinical evaluation of head motion correction on uMI Panorama PET/CT system

Fei Kang[1#], Zhaojuan Xie[1#], Wenhui Ma[1#], Zhiyong Quan[1], Guiyu Li[1], Kun Guo[1], Xiang Li[1], Taoqi Ma[1], Weidong Yang[1], Jing Wang[1]

[1] Department of Nuclear Medicine, Xijing Hospital, Fourth Military Medical University, Xi'an, China.

[#] These authors contributed equally to this article.

1. Introduction

Head motion (HM) during brain PET imaging poses significant challenges, introducing errors in uptake estimation and creating artifacts that compromise diagnostic accuracy. Advanced scanners, such as the uMI Panorama PET/CT (1), require minimal patient movement to achieve optimal spatial resolutions, including sub-3-mm full-width-half-maximum. In clinical settings where precise evaluations are critical for diagnosis, treatment planning, and assessing treatment responses, HM can undermine diagnostic confidence (2). Additionally, HM can lead to misalignment between PET and CT images, causing artifacts such as attenuation mismatches and localization issues. In extreme cases, significant motion blur may necessitate rescanning.

Traditional methods like frame-based image registration and hardware-based motion tracking (HMT) have limitations leading to artifacts (3-9). To address these limitations, data-driven HMC techniques have emerged (10,11). Methods like principal component analysis and centroid of distribution (COD) estimate rigid motion from PET raw data, offering software-based solutions easily integrated into clinical processes. The NeuroFocus[1] algorithm, specifically designed for the uMI Panorama PET/CT system, is a significant innovation. This system, equipped with a 189-picosecond time-of-flight (TOF) resolution and a 35-centimeter axial field of view (FOV), uses a statistics-based method developed by Revilla et al. to detect HM without parameter adjustments, accurately distinguishing COD variations caused by HM (12).

This study presents three key findings: (1) validating the precision of NeuroFocus for the uMI Panorama PET/CT system; (2) demonstrating the algorithm's effectiveness in diagnosing brain disorders; and (3) analyzing the frequency and severity of HM in clinical 18F-FDG brain studies. Further, this study marks the first large-scale clinical application of an HMC algorithm with short PET acquisition times.

2. Materials and Methods

2.1 Validation study data acquisition

The study involved 15 volunteers who participated in a prospective validation process. Each participant underwent a 3-minute brain PET scan on a single bed, conducted approximately 52.2±9.2 minutes after the administration of 18F-FDG. During the first scan, the volunteers were instructed to remain completely still ("NoMo"). For the second 3-minute scan, participants were directed to perform specific translational and rotational movements ("InstrMo"). Prior to each PET scan, a CT scan was performed for attenuation correction (AC). Additionally, MR images, including T1-weighted, contrast-enhanced T1-weighted, and T2-weighted images, were collected for each participant on the same day. The study, conducted at Xijing Hospital in Xi'an, China, was approved by the Ethics Committee of the Medical University in accordance with the revised Declaration of Helsinki (1964). All participants provided written informed consent.

2.2 Evaluation study data acquisition

A retrospective analysis was conducted on 302 clinical single-bed brain 18F-FDG scans, each lasting 3.0 minutes and performed 75.0±19.9 minutes after injection. The scans were classified into two groups: those without head motion correction (NMC) and those with head motion correction (HMC). Each study included a CT scan for attenuation correction (AC), though no MR images were obtained. Detailed patient information is provided in Table 1. The institutional review board approved this retrospective analysis, waiving the requirement for informed consent.

2.3 Head motion correction algorithm

[1]This product may not be available for such sales in some countries.

The head motion correction (HMC) algorithm involves three essential stages: motion detection, estimation, and correction. Motion was detected using the Center of Distribution (COD) algorithm, which produced a COD trace at 1 Hz intervals. By distinguishing motion-induced variations from statistical count variations in the COD trace, the study was divided into consecutive motion-free frames (MFFs), separated by motion time points. Frames shorter than 5 seconds were discarded. Motion estimation involved rigidly registering subsequent MFFs to a reference frame (the first MFF) using mutual information difference as the similarity metric. The first MFF was assumed to align spatially with the CT scan, ensuring no movement occurred between the CT and PET scans. The transformation matrix T(i) was used to estimate the i-th MFF, and the CT attenuation map was adjusted using the inverse of T(i) to create a matched attenuation map. Ordered subset expectation maximization with attenuation correction (OSEM-AC) was applied to each MFF, and all OSEM-AC MFFs were then transformed back to the reference frame and summed to produce the final HMC image. Reconstructions used a voxel size of 1.20×1.20×1.45 mm^3.

2.4 Evaluation

For the validation dataset, FreeSurfer was used to segment paired T1-weighted MR images into 109 brain regions of interest (ROIs), which were then resliced to match individual PET scans and grouped into 11 gray matter (GM) regions: amygdala, caudate, cerebellum cortex, frontal, hippocampus, insula, occipital, parietal, putamen, temporal, and thalamus. The percentage differences in standard uptake value (SUVmean) between the instructed motion (InstrMo) and no motion (NoMo) scans, as well as between InstrMo with HMC and NoMo, were reported for each GM region.

For the evaluation dataset, brain ROIs were created using an in-house CT-based segmentation algorithm. After registering with the MNI brain MRI template, 116 AAL brain ROIs were mapped to individual CT spaces. Cerebellum uptake and SUVmean ratio images were calculated, and a threshold was applied to create a binary GM mask. The cerebellum ROI was used to calculate cerebellum uptake on the reference frame using OSEM with AC. The SUVmean ratio image of the reference frame was generated with cerebellum uptake as the reference value, and a threshold of 1.0 was applied to create a binary GM mask. Overlapping regions between the mask and the 116 ROIs were used to refine GM regions, which were then merged into 11 regions based on the AAL definition. Supplemental Figure 1 illustrates the process for generating brain ROIs.

To quantify head motion, the distance traveled by each ROI was calculated through image registration, and the distances traveled by all 116 ROIs during different MFFs were averaged per minute. The average motion amplitude for the 11 combined GM ROIs was calculated by averaging the distances moved by the sub-ROIs, with reported distances of movement documented for each case study.

3. Results

3.1 Prospective validation study

Figure 1 presents three cases from the validation study, where significant image blurring is observed in the InstrMo scans due to head motion (HM). After applying the head motion correction (HMC), the images show a marked improvement in contrast and resolution, closely resembling the NoMo scans. The corresponding MR images also clearly depict anatomical structures in line with the NoMo studies. The detailed clinical diagnoses for these cases are provided in the caption of Figure 1.

Figure 2 highlights a patient from the evaluation study who was diagnosed with angioimmunoblastic T-cell lymphoma. This figure displays two axial slices from CT, NMC, and HMC images. The HMC images reveal areas of annular hypermetabolism with central hypometabolism in the left parietal lobe, as indicated by arrows, which were mostly blurred and indistinct in the NMC images due to HM.

In Figure 3, a case is shown where focal hypometabolism in the left thalamic and basal ganglia regions is clearly visible in the HMC image, while these regions are obscured by HM in the NMC image, making them undetectable.

Table 2 provides a quantitative analysis of the 15 validation studies, showing the SUVmean percentage error for each region of interest (ROI). The InstrMo scans generally demonstrated significant negative differences (-10%) with considerable variation across brain regions compared to NoMo scans. For example, the frontal region had a larger discrepancy (-16%) compared to the amygdala. After applying HMC, the differences were much smaller (around -1%) with

reduced variability (3%), indicating successful compensation for HM across all validation studies.

3.2 Retrospective evaluation study

Figure 4 shows two clinical evaluation studies of patients with suspected nervous system lymphoma and thalamic lacunar infarction. Significant HM was detected in the initial PET scans, which prompted the technician to recall the patients for re-scanning. During the second scans, both patients remained still. Remarkably, applying HMC to the initial scans resulted in images comparable to the re-scans, demonstrating the practical benefit of HMC in reducing the need for repeat scans due to HM.

Figure 5 illustrates a case of a patient with non-small cell lung cancer who exhibited significant involuntary head movements during both the initial and re-scan. Without advanced correction methods, these scans were not suitable for clinical diagnosis. However, after applying HMC, notable improvements in image resolution and contrast were observed in both sets of scans. The corrected images revealed reduced metabolic activity and swelling around a possible brain metastasis, which was only identifiable after using HMC.

In the evaluation study, Table 3 presents the numerical results of SUVmean changes across different brain regions after applying HMC. Participants were categorized into two groups based on the extent of head motion: small motion and large motion, using a 5% threshold in SUVmean change in the frontal lobe after HMC. In the small motion group, the average motion distance was relatively consistent across brain regions (2.4 mm) with low variability (1.9 mm). In contrast, the large motion group showed increased motion distances in all regions of interest (ROIs), ranging from 7.3 mm in the cerebellum to 15.0 mm in the frontal region, with significantly higher mean motion amplitude and variability (10.9 mm ±5.9 mm).

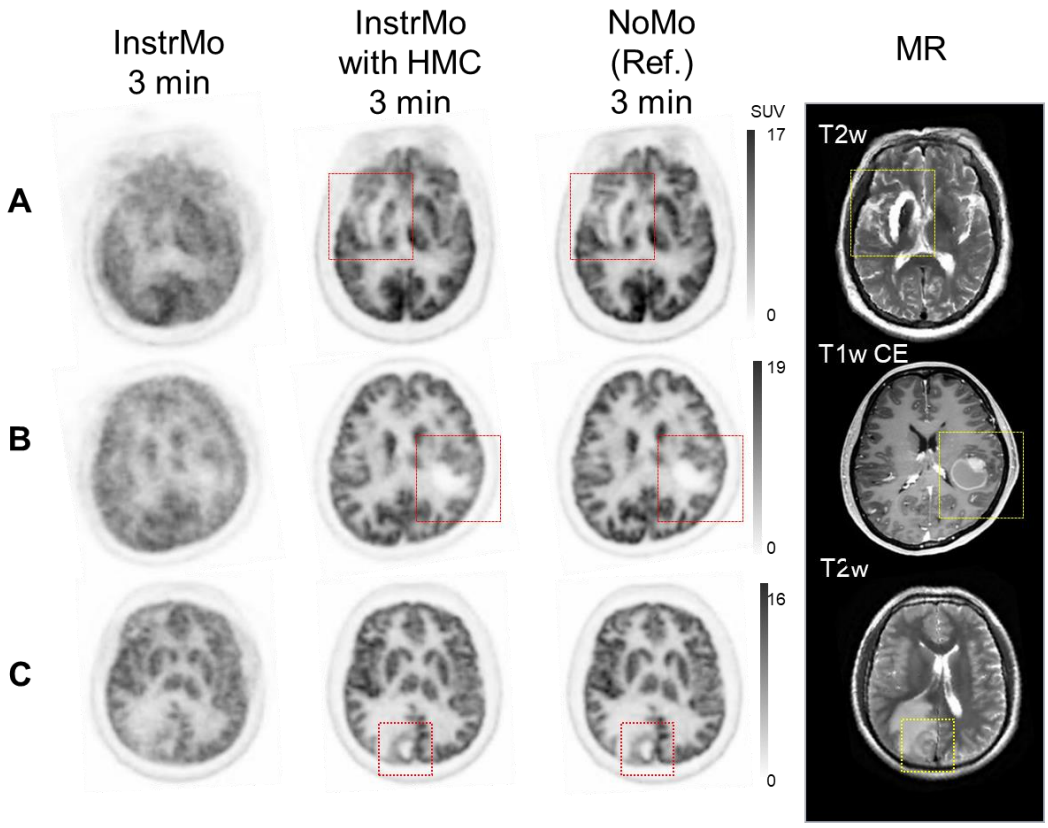

Figure 1. PET images from three distinct cases in the validation study, comparing scans with instructed motion (InstrMo), head motion correction (HMC), no motion (NoMo), and MRI. A) encephalomalacia/gliosis of the right basal ganglia and the right temporal lobe, and mild ex-vacuo dilatation of the right lateral ventricle in a geriatric patient with a history of right middle cerebral artery territory infarct; B) hypermetabolic nodules on PET aligns with nodular wall thickening in a cystic-appearing lesion observed in MR imaging associated with brain metastases from small-cell lung cancer; C) an annular hypermetabolic cerebral syphilitic gumma with surrounding edema in the right parietal occipital lobe. Averaged/maximal moving distance of the frontal lobe: 8.5/26.3 mm (Case A), 9.5/17.3 mm (B) and 19.0/54.2 mm (C). Injected dose/post injection/duration/body

weight: A) 273.8 MBq/56.1 min/3 min/69 kg, B) 214.6 MBq/65.6 min/3 min/56 kg and C) 270.1 MBq/67.8 min/3 min/70 kg. InstMo: instructed motion; HMC: instructed motion after head motion correction; NoMo: no motion repeat scan.

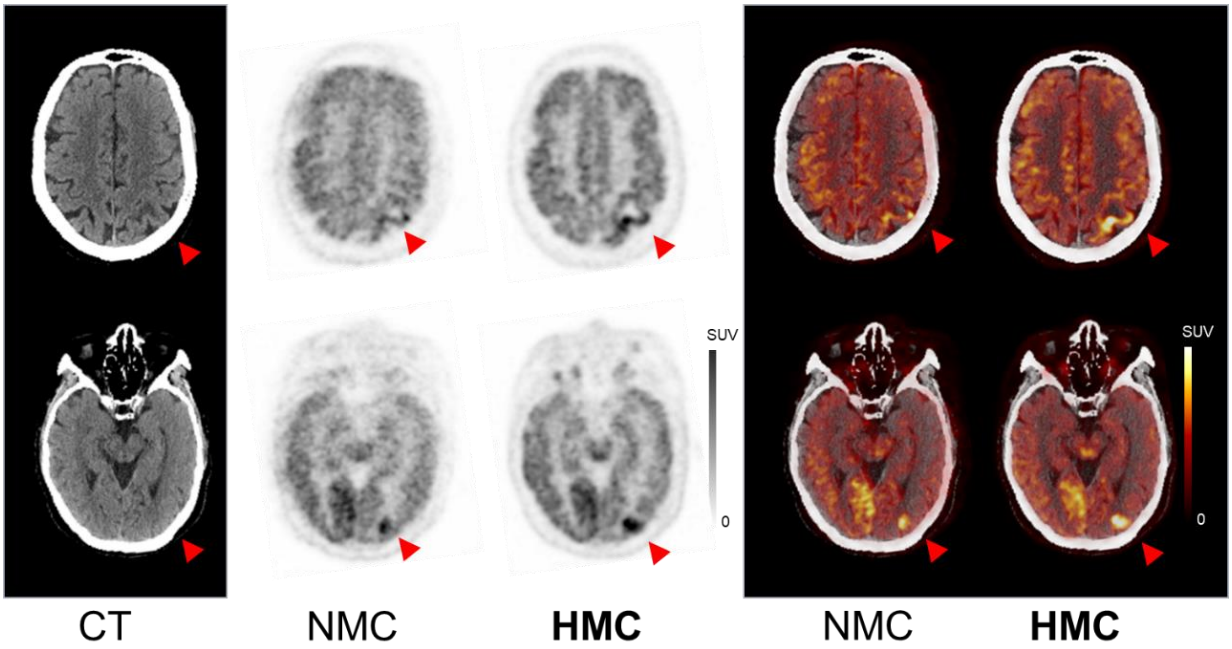

Figure 2. CT, PET and PET-CT with motion before and after HMC in a case of angioimmunoblastic T-cell lymphoma (AITL) suspected with cerebral infiltration due to acute onset of neurological symptoms. Motion blur and mis- registration were corrected after HMC. Areas of annular hypermetabolism with central hypometabolism in the left parietal lobe were revealed after HMC. Injected dose 251.6 MBq, post injection 90 min, frame duration 3 min single bed, body weight 65 kg. Averaged/maximal moving distance of the frontal lobe: 10.9/18.8 mm. NMC: no motion correction; HMC: head motion correction.

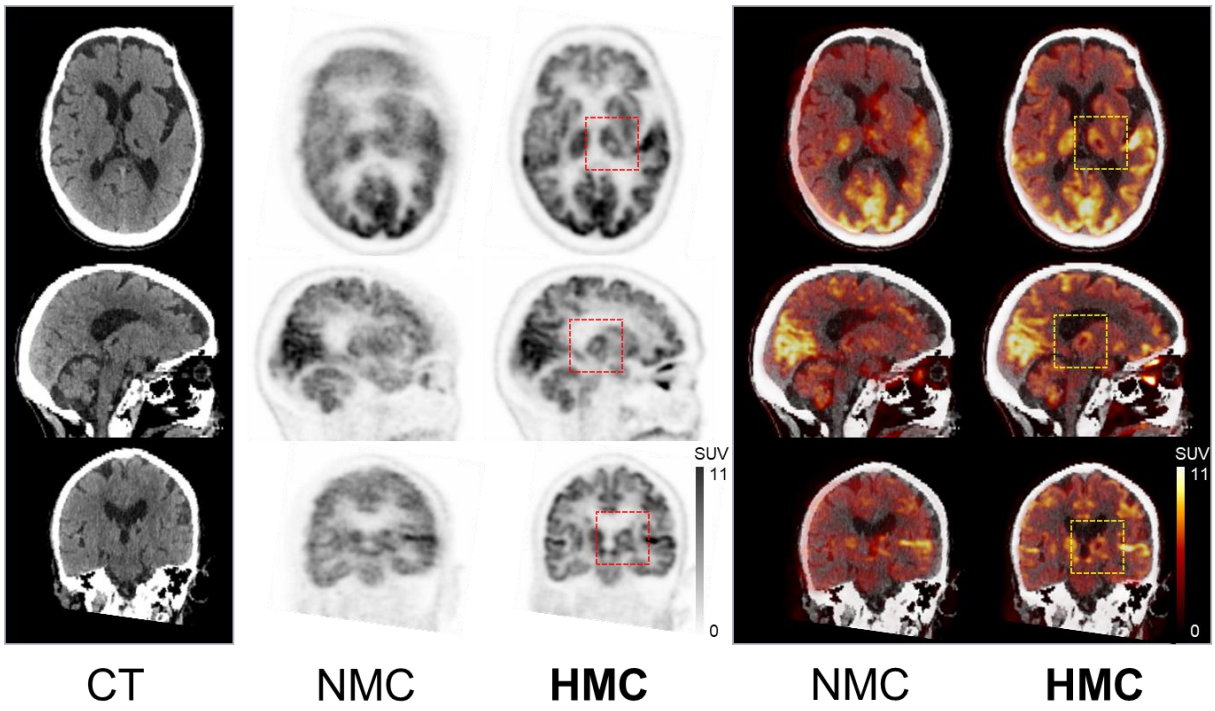

Figure 3. CT, PET and PET-CT with motion before and after HMC in a case of focal hypometabolism were observed in the left thalamic and basal ganglia region after HMC. Injected dose 229.4 MBq, post injection 69 min, frame duration 3 min, body weight 48 kg. Averaged/maximal moving distance of the frontal lobe: 13.7/25.4 mm. NMC: no motion correction; HMC: head motion correction.

4. Discussions

In this study, we performed both a prospective validation and a retrospective evaluation of the HMC algorithm from the uMI Panorama PET/CT scanner. The prospective validation included fifteen studies where participants were instructed to move their heads, while the retrospective evaluation examined 302 clinical brain studies using 18F-FDG, each with a 3-minute acquisition time. Results from the validation study showed that the HMC algorithm was highly effective, with an average quantitative error of less than 1% compared to scans without motion. In the retrospective evaluation, approximately 12% (38 out of 302) of clinical brain studies experienced significant head movement, underscoring the necessity of HMC. The effectiveness of the HMC algorithm was demonstrated across various brain diseases and clinical conditions, confirming its value in real-world applications. The reconstruction time for instructed motion studies averaged 11.0 ± 1.1 minutes, and reconstructions were submitted after acquisition. Across the evaluation studies, an average of 2.0 ± 9.7 seconds of data was discarded per case.

The European Association of Nuclear Medicine (EANM) guidelines emphasize the importance of neurological PET imaging in diagnosing cognitive and movement disorders, localizing epileptic foci, detecting neuro-infections, and assessing brain tumors. The guidelines recommend using small voxel reconstructions to improve brain structure visualization, which typically requires longer acquisition times to maintain adequate signal-to-noise ratios. For standard 18F-FDG brain scans, the guidelines suggest 10-15 minutes per bed position for scanners with short axial fields of view (FOV), with non-18F-FDG scans potentially requiring even longer times (up to 20-30 minutes per bed). However, using the high-sensitivity uMI Panorama scanner, we completed each clinical scan in just 3 minutes, maintaining sufficient image quality for diagnostic use. Despite the short scan duration, 12% of patients exhibited significant head movement, indicating that longer-duration scans may require an even greater reliance on HMC.

The introduction of HMC in PET imaging has significantly enhanced image quality and delivered practical benefits, including fewer rescan needs, reduced patient wait times, and improved comfort from repeated CT scans. The reduction in rescans also improves patient scheduling, streamlines workflows, and reduces the workload for healthcare professionals, optimizing resource management. HMC is particularly beneficial for patients who struggle to remain still during scans, reducing the need for tight head restraints or sedation, which improves both patient comfort and clinical efficiency.

This paper reviews key research efforts on HMC in PET imaging, comparing them to our proposed data-driven approach. One alternative is marker-less motion tracking using optical cameras. Spangler-Bickell et al. (2020) demonstrated this technique by attaching an optical camera to a PET/MR system's head coil, tracking head movement without markers using a curved forehead marker. Zeng et al. (2021) developed a marker-less system using stereovision cameras and infrared structured light to capture facial surfaces for motion tracking. Other researchers, such as Olesen and Kyme, have explored similar approaches, but these methods can be affected by facial expression changes and lack of thorough validation. Another approach used Microsoft's Kinect® system to track head motion, and recent studies by Zeng et al. (2021) applied neural networks to estimate motion between short frames, speeding up motion estimation. Further, deep learning techniques have been used to enhance PET image quality by generating high-count images from low-count data, which improves registration accuracy. Rezaei et al. (2018) proposed estimating rigid motion parameters using inertia tensors from TOF back projections. Each method offers distinct strategies for addressing HMC challenges in PET brain imaging, reflecting ongoing, diverse efforts in this critical area.

In conclusion, some limitations of the current HMC algorithm must be noted: 1) It is less effective for dynamic PET studies, as it does not track physiological changes over time; 2) It cannot correct motion between PET and CT acquisitions, leading to potential attenuation-related artifacts; and 3) It cannot correct continuous motion, such as tremors in

Parkinson's patients, due to its frame-based design. These limitations highlight the need for continuous advancements and innovations in HMC technology to improve the precision and utility of PET imaging.

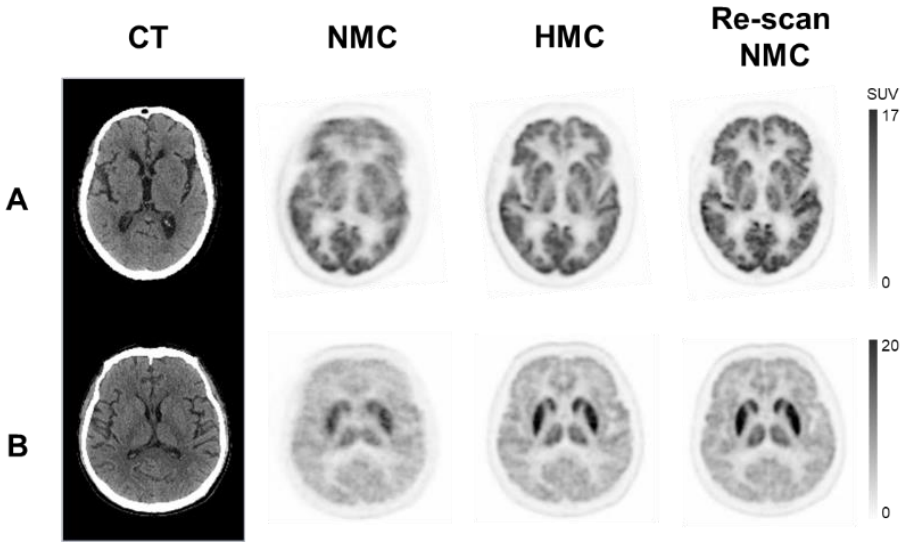

Figure 4. Comparison between PET with motion (NMC), after HMC and re-scan with minimal motion. Axial CT, PET with motion, with HMC, re-scan with minimal motion show A) hypometabolic foci in left thalamic indicating lacunar infarcts; B) bilateral hypermetabolism in the thalami and striatum in a patient with suspected nervous system lymphoma. Both HMC images are comparable to the re-scan images. A) Injected dose 266.4 MBq, post injection 71 min, frame duration 3 min, body weight 65 kg; B) Injected dose 366.3 MBq, post injection 66 min, frame duration 3 min, body weight 80 kg. Averaged/maximal moving distance of the frontal lobe: 9.6/47.2 mm (case A) and 10.0/16.0 mm (case B). NMC: no motion correction; HMC: head motion correction.

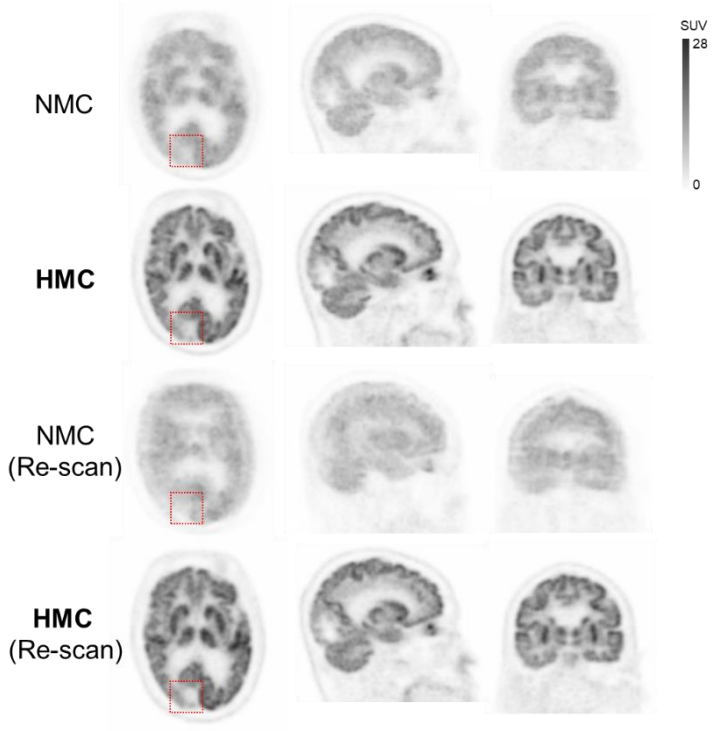

Figure 5. HMC and re-scan in cases with involuntary head movements. Images were corrupted by involuntary head motion in both the initial PET scan and the re-scan (NMC). Spatial resolution and contrast were significantly improved after HMC. The dotted box indicates the region of hypometabolic edema surrounding a suspected metastatic lesion in the occipital lobe in a patient with non-small cell lung cancer revealed after HMC. Injected dose 314.5 MBq, post injection 1st scan/re-scan 61/69 min, frame duration 3 min, body weight 77 kg. Averaged/maximal moving distance of the frontal lobe: 5.0/12.6 mm (1st scan) and 12.1/27.7 mm (re-scan). NMC: no motion correction; HMC: head motion correction.

Table 1. SUVmean change from NMC after HMC for the evaluation study (mean ±standard deviation (SD)) and mean motion distance for each brain region. NMC: no motion correction; HMC: head motion correction.

	Validation (w. MR)	Evaluation (w.o. MR)
Total participants	15	**302**
Age	34.1±13.1	**58.2±14.4**
Male	6	**171**
Female	**9**	**131**

Table 2. Validation study: % error in SUVmean as compared to the NoMo study. InstrMo: instructed motion; HMC: head motion correction

ROI	NoMo SUVmean	InstrMo (% error)	InstrMo with HMC (% error)
Amygdala	4.4±0.5	-4.3±4.7	**-0.1±1.8**
Caudate	6.6±1.2	-14.9±8.4	**-2.8±5.4**
Cerebellum	5.6±0.8	-5.6±3.2	**-2.2±1.5**
Frontal	6.8±0.9	-16.3±5.3	**-1.0±3.8**
Hippocampus	4.9±0.7	-2.4±5.3	**0.7±4.4**
Insula	5.6±0.7	-5.0±3.6	**-0.2±2.8**
Occipital	7.9±1.1	-13.9±3.7	**-3.1±4.2**
Parietal	6.6±0.9	-14.1±4.7	**0.5±3.6**
Putamen	7.3±1.3	-12.1±7.7	**-0.3±2.2**
Temporal	6.0±0.7	-11.3±5.8	**-0.1±3.7**
Thalamus	6.4±0.9	-11.1±4.8	**-0.2±1.4**
Mean average	6.2	-10.1	**-0.8**
SD average	**0.9**	**5.2**	**3.2**

Table 3. . SUVmean change from NMC after HMC for the evaluation study (mean ±standard deviation (SD)) and mean motion distance for each brain region. NMC: no motion correction; HMC: head motion correction.

	Small motion (N=264)		Large motion (N=38)	
ROI	**Mean motion distance / mm**	**SUVmean change / %**	**Mean motion distance / mm**	**SUVmean change / %**
Amygdala	2.5±1.9	0.4±2.6	11.8±6.3	**19.9±20.8**
Caudate	2.6±2.0	0.6±2.6	12.7±7.0	**22.9±13.7**
Cerebellum	2.1±1.7	-0.2±0.7	7.3±3.9	**2.9±3.7**
Frontal	2.9±2.0	0.3±1.3	15.0±8.1	**12.9±8.3**
Hippocampus	2.3±1.8	-0.3±1.4	10.1±5.3	**10.6±9.0**
Insula	2.6±1.9	0.1±1.1	13.0±7.0	**10.0±6.2**
Occipital	2.2±1.7	-0.2±0.7	6.7±4.4	**2.9±3.9**
Parietal	2.4±1.8	-0.0±0.8	9.5±5.2	**6.8±6.0**

Putamen	2.5±1.9	0.3±1.3	12.4±6.7	**12.2±10.4**
Temporal	2.5±1.8	0.1±1.0	11.8±6.2	**10.0±8.1**
Thalamus	2.2±1.8	-0.1±0.8	9.9±5.3	**8.2±7.8**
Mean average	**2.4**	**0.1**	**10.9**	**10.9**
SD average	**1.9**	**1.3**	**5.9**	**8.9**

5. Conclusion

A clinical study was conducted with fifteen participants to assess the accuracy of the NeuroFocus HMC algorithm on the uMI Panorama PET/CT system, using 18F-FDG in the evaluation process. During validation, where participants were instructed to perform head movements, the post-HMC standardized uptake value (SUV) error was found to be minimal, averaging -1±3% across all brain regions and participants. This represents a significant improvement from the previous error rate of -10±5% before applying HMC. In a broader analysis of 302 participants, approximately 12% of short-duration (3-minute) clinical brain scans showed substantial issues requiring correction. The HMC algorithm demonstrated strong efficacy in mitigating HM across various brain disorders, highlighting its potential for clinical use in brain research involving 18F-FDG.

6. Acknowledgement

The authors extend their gratitude to Chen Xi, Yue Li, Hao Liu, and Lei Shi for supporting NeuroFocus software and data acquisition. Special thanks are due to Enette Mae Revilla and Duo Zhang for manuscript editing. The authors thank Bingbing Zhao, Wenjun Yu, and Fenggang Jia for their support with the image processing software.

7. References

1. Li G, Ma W, Li X, Yang W, Quan Z, Ma T, Wang J, Wang Y, Kang F, Wang J. Performance Evaluation of the uMI Panorama PET/CT System in Accordance with the National Electrical Manufacturers Association NU 2-2018 Standard. J Nucl Med. 2024 Feb 22.
2. Polycarpou I, Soultanidis G, Tsoumpas C. Synergistic motion compensation strategies for positron emission tomography when acquired simultaneously with magnetic resonance imaging. Philos Trans A Math Phys Eng Sci. 2021;379:20200207.
3. Rahmim A, Dinelle K, Cheng JC, et al. Accurate event-driven motion compensation in high- resolution PET incorporating scattered and random events. IEEE Trans Med Imaging. 2008;27:1018- 1033.
4. Picard Y, Thompson CJ. Motion correction of PET images using multiple acquisition frames. IEEE Trans Med Imaging. 1997;16:137-144.
5. Montgomery AJ, Thielemans K, Mehta MA, Turkheimer F, Mustafovic S, Grasby PM. Correction of head movement on PET studies: comparison of methods. J Nucl Med. 2006;47:1936-1944.
6. Herzog H, Tellmann L, Fulton R, et al. Motion artifact reduction on parametric PET images of neuroreceptor binding. J Nucl Med. 2005;46:1059-1065.
7. Fulton RR, Meikle SR, Eberl S, Pfeiffer J, Constable C, Fulham MJ. Correction for head movements in positron emission tomography using an optical motion tracking system. IEEE Nuclear Science Symposium. Vol 3; 2000.
8. Costes N, Dagher A, Larcher K, Evans AC, Collins DL, Reilhac A. Motion correction of multi-frame PET data in neuroreceptor mapping: simulation based validation. Neuroimage. 2009;47:1496-1505.
9. Bloomfield PM, Spinks TJ, Reed J, et al. The design and implementation of a motion correction scheme for neurological PET. Phys Med Biol. 2003;48:959-978.
10. Thielemans K, Schleyer PJ, Dunn JT, Marsden PK, Manjeshwar RM. Using PCA to detect head motion from

pet list mode data. IEEE Nuclear Science Symposium and Medical Imaging Conference; 2013.

11.Schleyer PJ, Dunn JT, Reeves S, Brownings S, Marsden PK, Thielemans K. Detecting and estimating head motion in brain PET acquisitions using raw time-of-flight PET data. Phys Med Biol. 2015;60:6441-6458.

12.Revilla EM, Gallezot JD, Naganawa M, et al. Adaptive data-driven motion detection and optimized correction for brain PET. Neuroimage. 2022;252:119031.

Author Biography

Prof. Jing Wang

Director, Department of Nuclear Medicine

Xijing Hospital, China

Prof. Jing Wang is a distinguished professor and chief physician, currently serving as Director of the Department of Nuclear Medicine at Xijing Hospital and a graduate advisor at the Fourth Military Medical University. With a medical degree and Ph.D. from the Fourth Military Medical University, Prof. Wang has over 30 years of experience in nuclear medicine, specializing in oncological molecular nuclear imaging and multimodal imaging applications. She has led numerous high-impact research projects, including key National Natural Science Foundation of China (NSFC) projects, and published over 50 SCI-indexed articles, with her work earning notable recognition, such as the 2018 First Prize for Science and Technology Progress in Shaanxi Province.

Prof. Wang holds several prominent professional roles, including Chair-elect of the Chinese Society of Nuclear Medicine and Expert Consultant for the Central Military Commission's Health Committee. Her contributions to nuclear medicine have been widely recognized, with accolades like the "Chinese Nuclear Medicine Physician Award" and the “Outstanding Physician for Exceptional Achievements” award. She is also Deputy Editor of the Chinese Journal of Nuclear Medicine and Molecular Imaging and has authored multiple textbooks, advancing both clinical practice and research in nuclear medicine.

PASSION for CHANGE

If you have any questions about the magazine, or simply wish to reach out to us for any other reasons, you are welcomed to contact us at the following email address: compliance@united-imaging.com